Nondegenerate parametric interactions and nonclassical effects

A. Bandilla,[1] G. Drobný,[2] and I. Jex[1,2]
[1]*Arbeitsgruppe "Nichtklassische Strahlung" der Max-Planck-Gesellschaft an der Humboldt-Universität Berlin, Rudower Chaussee 5, Haus 10.16, 12484 Berlin, Germany*
[2]*Institute of Physics, Slovak Academy of Sciences, Dúbravská cesta 9, 842 28 Bratislava, Slovakia*
(Received 24 May 1995)

We consider the classical and quantum-mechanical processes of three-wave interactions in different phase regimes and present numerical calculations for the quantum case, where all three modes are sizably excited from the beginning. These excitations are coherent so that various important phase regimes can be adjusted. In addition, one mode can also be prepared in a squeezed or Kerr state. The classical solutions are well known and are briefly summarized, but certain phase regimes are classically unexplored and we show here that they give interesting and surprising results. In the out-of-phase regime (where the photon numbers do not change in the first order of time) we get, with an initial Kerr state, strongly sub-Poissonian photon statistics in the signal after a short interaction time. This effect is limited by the classically described phase shifts that are present even in the parametric approximation. This nonclassical phenomenon (due to the Kerr state) helps us to understand similar nonclassical effects generated by entangled states of the pump and signal during sum-frequency generation.

PACS number(s): 42.50.Dv

I. INTRODUCTION

The parametric interaction between intense light waves has been studied since the laser came into existence in 1960. Shortly after the creation of the second harmonic of the laser light had been observed by Franken *et al.* [1], a comprehensive paper by Armstrong *et al.* appeared [2] that describes three-wave and four-wave interactions in nonlinear media and gives exact solutions for the classical coupled-mode equations. This work shows the great importance of coherence effects during nonlinear interactions and is now at the heart of nonlinear optics and also the basis of many quantum optical investigations. Let us confine ourselves to three interacting waves, i.e., $\chi^{(2)}$ media, and consider the general case that all waves are excited at the beginning of the interaction. In the case of exact resonance we have the relation

$$\omega_3 = \omega_1 + \omega_2 , \tag{1}$$

where ω_3 is the frequency of the pump and ω_1 and ω_2 are the same frequencies of the signal and idler, respectively. We assume phase matching of the wave vectors, which provides the justification for retaining only these three waves or three modes in the quantum case.

An important approximation that allows an analytic solution also in the quantum case is the so-called parametric one, where the strong pump wave is treated as a c number and any depletion is neglected while the relatively weak signal and idler can change considerably [3]. Thereby we get the linear parametric amplifier (for the signal), which can be phase insensitive (with the idler mode initially empty) or phase dependent (with the idler initially coherently excited). Experimentally the latest achievement is a quantum noise reduction in such an amplifier by coupling a squeezed vacuum into the idler mode, performed by Ou *et al.* [4]. Another property of signal and idler photons within the parametric approximation is their strong correlation, allowing many experiments in respect to fundamental questions of interference. Pioneering investigations in this field were made by Wang *et al.* (cf., e.g., [5]). Finally, we should remark that the parametric approximation is easily applied, but its justification is hard to show [6]. Most quantum optical investigations with $\chi^{(2)}$ media are carried out in this approximation [7].

However, an arbitrary preparation of all three waves is now experimentally possible with different phase relations between them. Classically the solutions are then well known, but quantum mechanically we have to resort to numerical methods [8]. In their first calculations Walls and Barakat started with a Fock state in the pump mode or Fock states in the pump and signal. By now these initial states have been replaced by coherent states with considerable excitation, but at least one mode is still in the vacuum. During the interaction the vacuum mode becomes excited and its phase adjusts automatically to the right phase difference. Thus, the manifold of phase relations cannot be explored with two excited coherent states either.

Here we present analytical and numerical calculations for the quantum case, where all three modes are considerably excited from the beginning, and choose a proper phase relation between them. A coherent state with a mean photon number exceeding 5 already has a sufficiently sharp mean phase [9]. Hence, starting with such states in all three modes allows therefore the choice of an arbitrary initial phase relation between them for the nondegenerate three-wave interaction. This is compared with classical solutions and applied to a specially prepared signal, which under sum-frequency generation shows strong sub-Poissonian photon statistics. The results of this approach in turn help us understand the nonclassical properties occurring during sum-frequency generation for coherent initial states after a quasiperiod.

II. QUANTUM THEORY OF THREE-WAVE INTERACTION

We start with the Hamiltonian for the nondegenerate three-wave interaction in the interaction picture

$$\hat{H}_{\rm int}=\hbar\kappa(\hat{a}\hat{b}\hat{c}^{\dagger}+\hat{a}^{\dagger}\hat{b}^{\dagger}\hat{c}), \tag{2}$$

where $\hat{c}$ ($\hat{c}^{\dagger}$) is the annihilation (creation) operator of the pump mode (frequency ω_3) and $\hat{a}$ and $\hat{b}$ denote the corresponding operators for the signal and idler, respectively. The coupling constant κ contains the nonlinear susceptibility $\chi^{(2)}$. Because the system (2) can only be numerically solved by diagonalization, we limit our analytical treatment to a short-time expansion. For the signal mode operator we find up to second order in κt, from the Heisenberg equations of motion,

$$\hat{a}(t)=\hat{a}-i\kappa t\hat{b}^{\dagger}\hat{c}+\frac{(\kappa t)^2}{2!}(\hat{c}^{\dagger}\hat{a}\hat{c}-\hat{b}^{\dagger}\hat{a}\hat{b})+O((\kappa t)^3), \tag{3}$$

where all operators without a time argument are taken at $t=0$. Equivalent expressions can be written for $\hat{b}$ and $\hat{c}$. The photon number in the signal is then described by

$$\begin{aligned}\hat{a}^{\dagger}(t)\hat{a}(t)=&\hat{a}^{\dagger}\hat{a}-i\kappa t(\hat{a}^{\dagger}\hat{b}^{\dagger}\hat{c}-\hat{c}^{\dagger}\hat{b}\hat{a})\\&+(\kappa t)^2[\hat{c}^{\dagger}\hat{c}(\hat{a}^{\dagger}\hat{a}+\hat{b}\hat{b}^{\dagger})-\hat{a}^{\dagger}\hat{a}\hat{b}^{\dagger}\hat{b}]\\&+O((\kappa t)^3).\end{aligned} \tag{4}$$

Assume now initially coherent states in all three modes

$$|\alpha\rangle_a|\beta\rangle_b|\gamma\rangle_c,$$

$$\alpha=|\alpha|e^{i\varphi_a},\quad \beta=|\beta|e^{i\varphi_b},\quad \gamma=|\gamma|e^{i\varphi_c}. \tag{5}$$

Then the expectation value of (4) results in

$$\begin{aligned}\langle\hat{a}^{\dagger}(t)\hat{a}(t)\rangle=&|\alpha|^2+2\kappa t|\alpha||\beta||\gamma|\sin(\varphi_c-\varphi_b-\varphi_a)\\&+\kappa^2t^2[|\gamma|^2(|\alpha|^2+|\beta|^2+1)-|\alpha|^2|\beta|^2]\\&+O(\kappa^3t^3).\end{aligned} \tag{6}$$

We call the linear terms in κt coherent because they depend on the phase difference. If $\Delta\varphi=\varphi_c-\varphi_b-\varphi_a=-\pi/2$ the signal becomes attenuated while for $\Delta\varphi=\pi/2$ the signal is first amplified. In addition, we consider the phase difference $\Delta\varphi=0$, where all phase-dependent terms in (6) disappear and the direction of the process is given simply by the intensity relations (the second-order term). We call this initial condition the out-of-phase regime. Note further that the fluctuations enter (4) in the second-order term by the commutation relation of the idler operators. If we neglect this fluctuation contribution, the condition for the disappearance of the second-order term in (6) is

$$|\gamma|^2=\frac{|\alpha|^2|\beta|^2}{|\alpha|^2+|\beta|^2}. \tag{7}$$

For such intensity relations and $\Delta\varphi=0$ there is classically no energy exchange, as will be discussed later. Before deriving the classical equations and showing the numerical results, let us also provide the squared number operator

$$\begin{aligned}[\hat{a}^{\dagger}(t)\hat{a}(t)]^2=&\hat{a}^{\dagger2}\hat{a}^2+\hat{a}^{\dagger}\hat{a}+i2\kappa t(\hat{a}^{\dagger}\hat{a}^2\hat{c}^{\dagger}\hat{b}-\hat{a}^{\dagger2}\hat{a}\hat{b}^{\dagger}\hat{c})+i\kappa t(\hat{a}\hat{c}^{\dagger}\hat{b}-\hat{a}^{\dagger}\hat{b}^{\dagger}\hat{c})+(\kappa t)^2[2(\hat{c}^{\dagger}\hat{c}-\hat{b}^{\dagger}\hat{b})(\hat{a}^{\dagger2}\hat{a}^2+\hat{a}^{\dagger}\hat{a})\\&+2\hat{c}^{\dagger}\hat{c}(\hat{b}^{\dagger}\hat{b}+1)\hat{a}^{\dagger}\hat{a}]-(\kappa t)^2[\hat{c}^{\dagger2}\hat{a}^2\hat{b}^2+\hat{c}^2\hat{b}^{\dagger2}\hat{a}^{\dagger2}-2\hat{a}^{\dagger}\hat{a}\hat{c}^{\dagger}\hat{c}\hat{b}^{\dagger}\hat{b}-\hat{a}^{\dagger}\hat{a}\hat{b}^{\dagger}\hat{b}-\hat{c}^{\dagger}\hat{c}(\hat{a}^{\dagger}\hat{a}+\hat{b}^{\dagger}\hat{b}+1)]\\&+O((\kappa t)^3).\end{aligned} \tag{8}$$

In (8) all single-mode operators are in normal order. This simplifies the calculation of the variance of the photon number considerably. Special attention will be dedicated to terms of the first order of time in (8). For three coherent states the disappearance of the first-order terms in (6) would result in the same effect in the expectation value of (8). However, for more general states, we can set these terms equal to zero in the photon number and nevertheless retain nonzero terms for the expectation value of (8). This could give a strong tendency to sub-Poissonian statistics. Note two possibilities for this in the expectation value of the first-order term of (8). First, there are higher moments of $\hat{a},\hat{a}^{\dagger}$ and second, due to some entanglement, any factorization of the expectation values of the different modes may become impossible. We will discuss both properties, but focus on the first.

Finally, we should point out that there is another peculiarity in (8) that affects the nonclassical properties of the signal and idler and has no analog within the parametric approximation: If we assume for the pump a squeezed vacuum, then the first-order terms in the expectation values of (4) and (8) would vanish, but the ensemble average of the term in the last set of square brackets in (8) shows that the squeezed pump can determine tendencies as well. If the signal and idler are initially in coherent states with real amplitudes α and β, then

$$[2\langle\hat{c}^{\dagger}\hat{c}\rangle-\langle\hat{c}^2\rangle-\langle\hat{c}^{\dagger2}\rangle]\alpha^2\beta^2$$

can be positive or negative, depending on the phase of the pump squeezing. This effect can be enhanced by increasing α and β. On the other hand, the signal and idler generate the sum frequency that changes in turn the pump field. This effect can now be calculated numerically and will be discussed elsewhere.

III. CLASSICAL DESCRIPTION OF THE THREE-WAVE INTERACTION

Because we will mainly investigate the case $\Delta\varphi=0$ (with no coherent interaction at the beginning) and this is normally avoided even in the classical coupled-mode equations [2], we should also briefly discuss the classical interaction. Introduc-

ing a scaled time $\zeta=\kappa t$, we get, for the classical amplitudes, the equations [2]

$$\frac{du_1}{d\zeta}=-u_2u_3\ \sin\theta,$$

$$\frac{du_2}{d\zeta}=-u_1u_3\ \sin\theta,$$

$$\frac{du_3}{d\zeta}=u_2u_1\ \sin\theta, \tag{9}$$

where u_1,u_2,u_3 are the classical (slowly varying) amplitudes of the signal, idler, and pump, respectively, and

$$\theta(\zeta)=\phi_3(\zeta)-\phi_2(\zeta)-\phi_1(\zeta) \tag{10}$$

is the phase difference between the phase of these three waves. The equation of motion for $\theta(\zeta)$ is

$$\frac{d\theta}{d\zeta}=\frac{\cos\theta}{\sin\theta}\frac{d}{d\zeta}\ \ln(u_1u_2u_3). \tag{11}$$

We neglect here any mismatch and mention that there are three constants

$$m_1=u_2^2+u_3^2,\quad m_2=u_1^2+u_3^2,\quad m_3=u_1^2-u_2^2, \tag{12}$$

which constitute the so-called Manley-Rowe relations and have their corresponding conserved quantities in the quantum system described by (2). There is also the conservation of power flow and we can interpret u_1^2,u_2^2,u_3^2 as photon numbers in the corresponding modes if we introduce a suitable rescaling of the u_i and ζ [10], which does not change the form of the equations in any way. Thus Eqs. (9) and (11) are the classical equivalents of the Heisenberg equations of motion derived from (2).

The advantage of Eq. (11) for the phase difference is that it can immediately be integrated to give

$$u_1(\zeta)u_2(\zeta)u_3(\zeta)\cos[\theta(\zeta)]=\Gamma =u_1(0)u_2(0)u_3(0)\cos[\theta(0)]. \tag{13}$$

Note, however, that the single equations for each phase

$$\frac{d\phi_1}{d\zeta}=\frac{u_2u_3}{u_1}\cos\theta,$$

$$\frac{d\phi_2}{d\zeta}=\frac{u_1u_3}{u_2}\cos\theta,$$

$$\frac{d\phi_3}{d\zeta}=\frac{u_2u_1}{u_3}\cos\theta \tag{14}$$

are not solved by this approach.

With the help of (13) and (12) the system (9) can then be integrated, which results in the well-known Jacobian elliptic functions for the $u_i^2(\zeta)$ $(i=1,2,3)$ that correspond to the photon numbers. With the help of these solutions and Γ we can study the motion of $\cos\theta(\zeta)$ and of $\theta(\zeta)=\phi_3(\zeta)-\phi_2(\zeta)-\phi_1(\zeta)$, but for the motion of each single phase we have to integrate (14). This will be discussed in more details in [11]. Here we will gain insight into the behavior of each single phase by calculating the Q functions in the quantum picture.

The solutions of (9) depend decisively on the constant Γ given in (13), which appears in the cubic equation

$$x^3-(m_2+m_1)x^2+m_2m_1x-\Gamma^2=0, \tag{15}$$

where $x=u_3^2$ and (15) always has three real roots. It is easy to solve (15) for $\Gamma=0$ [where $\Delta\varphi=\pm\pi/2$, or one $u_i(0)=0$ $(i=1,2,3]$, but the solution for $\Gamma\neq0$ is just as simple. For the case $\Gamma=u_1(0)u_2(0)u_3(0)$ $[\cos\theta(0)=1]$ we find as the first root

$$x_1=u_3^2(0) \tag{16}$$

and factor it out so that we are left with a quadratic equation. The three roots have to be ordered [2] and their magnitude and mutual relations determine whether or not the signal first increases for $\Delta\varphi=0$. To illustrate this we calculate also the other roots to

$$x_{2,3}=\frac{1}{2}\{u_3^2(0)+u_2^2(0)+u_1^2(0) \pm\sqrt{[u_3^2(0)+u_2^2(0)+u_1^2(0)]^2-4u_1^2(0)u_2^2(0)}\}. \tag{17}$$

By setting the roots

$$u_{3c}^2\geqslant u_{3b}^2\geqslant u_{3a}^2\geqslant0$$

and introducing the constant

$$m=\frac{u_{3b}^2-u_{3a}^2}{u_{3c}^2-u_{3a}^2}, \tag{18}$$

the photon numbers of the three waves behave as

$$u_3^2(\zeta)=u_{3a}^2+(u_{3b}^2-u_{3a}^2)sn^2[(u_{3c}^2-u_{3a}^2)^{1/2}(\zeta+\zeta_0),m],$$

$$u_2^2(\zeta)=u_2^2(0)+u_3^2(0)-u_3^2(\zeta),$$

$$u_1^2(\zeta)=u_1^2(0)+u_3^2(0)-u_3^2(\zeta). \tag{19}$$

In (19) we denoted by $\mathrm{sn}[u,m]$ the Jacobian elliptic function and by m its parameter [12] and used the conserved quantities m_1 and m_2 [Eq. (12)] to express the signal and idler intensity by the intensity of the pump. The constant ζ_0 has to be determined from the initial conditions. As a numerical example we consider now

$$u_1^2(0)=36,\ u_2^2(0)=16,\ u_3^2(0)=9 \tag{20}$$

(these values will also be taken for our quantum calculations) and find then

$$u_{3a}^2=9,\ \ u_{3b}^2=11.68,\ \ u_{3c}^2=49.32. \tag{21}$$

From (19) and (20) it follows that $\zeta_0=0$. Looking at the difference $u_{3b}^2-u_{3a}^2$, we conclude that the energy exchange is strongly limited. It can even be completely suppressed

(classically) for $u_{3b}^2 \to u_{3a}^2$, which amounts to condition (7). No energy exchange would be reached in our example for

$$u_1^2(0)=36,\ u_2^2(0)=16,\ u_3^2(0)=11.077. \tag{22}$$

Comparing (22) and (20) one can see how close the photon numbers (20) are to the no-exchange case. It is instructive to add another example

$$u_1^2(0)=16,\ u_2^2(0)=9,\ u_3^2(0)=36. \tag{23}$$

Then we find the roots to be

$$u_{3a}^2=2.46,\ \ u_{3b}^2=36,\ \ u_{3c}^2=58.54 \tag{24}$$

and here the energy exchange is almost as complete as for optimum phases [$\Gamma=0$, where $\theta(0)=\pm\pi/2$, or one $u_i^2(0)=0$ $(i=1,2,3)$]. We conclude that in this out-of-phase regime, the amount of the pump intensity in relation to the signal and idler intensity determines how complete the energy exchange can be and emphasize that for this start the phase difference does not stay at $\theta=0$ $(\Delta\varphi=0)$. Contrarily, it changes in the direction that favors the energy exchange. Simultaneously the single phases change much faster [11]. In the next section we will compare these classical results with quantum calculations for coherent input states and then turn to nonclassical peculiarities.

IV. APPLICATION TO COHERENT INPUT STATES

The quantum-mechanical equivalent of (13) is the expectation value of the interaction Hamiltonian (2). Hence the subtle classical results have their quantum-mechanical analogs in the solution of (2). Especially from $\Gamma=0$ we can conclude that $\langle\hat{H}_{\rm int}\rangle=0$ and classically this requires that $\cos[\theta(\zeta)]$ remains zero for all ζ because all amplitudes can become nonzero [see (13)]. From the equations for the single phases (14) it follows then that the single phases stay at constant values. To determine the phases quantum mechanically we can calculate the phase probability distributions and with the help of them calculate the average phase values, which behave in approximately the same way as the classical phases if we are sufficiently far away from the phase jump points. Things are different for $\Gamma\neq 0$ because then $\cos[\theta(\zeta)]$, along with the amplitudes cannot become zero. However, $\sin[\theta(\zeta)]$ can change its sign and reverse the power flow in Eqs. (9) because now the phases move within certain limits. The quantum-mechanical expectation values of the phase (e.g., via the Pegg-Barnett approach [13]) can again be determined by means of the phase distribution function. Instructive insight into this phase behavior has already been delivered by the contour lines of the Q function, to which we will limit ourselves in this paper. A more detailed discussion of the different phase regimes will be given in [11].

Here we illustrate these facts by our numerical results and show then the nonclassical features. Figure 1(a) demonstrates the behavior of the signal photon number for the initial state (5) with $|\alpha|=6$, $|\beta|=4$, and $|\gamma|=3$. Note that the period of the energy exchange is almost the same as for both $\Delta\varphi=0$ and $\Delta\varphi=-\pi/2$, even though the amplitude parameters prevent a sizable energy transfer for $\Delta\varphi=0$. For sufficiently intense coherent states we can identify $\theta(0)=\phi_3(0)-\phi_1(0)-\phi_2(0)=0$ with $\Delta\varphi=\varphi_3-\varphi_1-\varphi_2=0$. Both processes ($\Delta\varphi=0$ and $\Delta\varphi=\pi/2$) start with sum-frequency generation, but the Q parameter of the signal

$$Q=\frac{\langle(\hat{a}^\dagger\hat{a})^2\rangle-\langle\hat{a}^\dagger\hat{a}\rangle^2}{\langle\hat{a}^\dagger\hat{a}\rangle}-1, \tag{25}$$

plotted in Fig. 1(b), becomes negative only after the second start of sum-frequency generation, showing strongly sub-Poissonian behavior of the signal in the case $\Delta\varphi=-\pi/2$. This phenomenon is at the center of our paper because it represents a very interesting nonclassical effect that occurs unexpectedly in sum-frequency generation. The phase-stable motion of the contour lines of the Q function for the signal is plotted in Fig. 1(c). We call a motion phase stable when the center of these contour lines shifts only radially. Note the remarkable deformation of the Q function when sum-frequency generation drives the nonlinearly amplified signal into sub-Poissonian photon statistics.

The sum-frequency generation in the first quasiperiod is for both the signal and idler only a one-photon process and therefore not so different from a simple reduction by absorption (if both modes start with coherent inputs). However, the spontaneous decay of pump photons increases the fluctuations in the signal and idler visible as a blowup of the contour lines in Fig. 1(c). These phenomena have their analogs in the parametric approximation, which will be discussed later. When the idler amplitude crosses zero there is a phase jump but no saturation because also this zero passage of the idler amplitude finds its equivalent within the parametric approximation. After this phase jump, the signal and idler are amplified and this process becomes increasingly nonlinear because the pump is affected by its depletion. Only the exhaustion of the pump is characterized by strong saturation and prepares the signal into a different state for the restart of sum-frequency generation. The character of this state that shows enhanced phase fluctuations [cf. Fig. 1(c)] will become clear in the following.

Analogous effects were observed with the initial conditions

$$|\alpha\rangle_a|0\rangle_b|\gamma\rangle_c,\ \ |\alpha\rangle_a|\beta\rangle_b|0\rangle_c, \tag{26}$$

where the initial coherent amplitudes could be as high as $\alpha=\gamma=8$ starting with difference-frequency generation [14] and $\alpha=9,\beta=5$ generating first sum frequency [15]. The phases in the newly generated modes in (26) adjust in a way that corresponds to $\Delta\varphi=\pm\pi/2$, respectively.

For completeness and further illustration we present in Figs. 2(a) and 2(b) results corresponding to Fig. 1, but now with $\Delta\varphi=\pi/2$. Hence, here the interaction starts with difference-frequency generation (or phase-dependent amplification). After total depletion of the pump the process reverses and the signal and idler are used to establish the pump (sum frequency). A weak sub-Poissonian effect of the Q parameter is thereby observed, but the preparation was not long enough to result in a strong narrowing. This is only reached at the second start of the signal and idler depletion in Fig. 2.

Another important case is met when the pump wave becomes the strongest mode. An example that corresponds to the photon numbers in (23) is illustrated in Figs. 3 and 4.

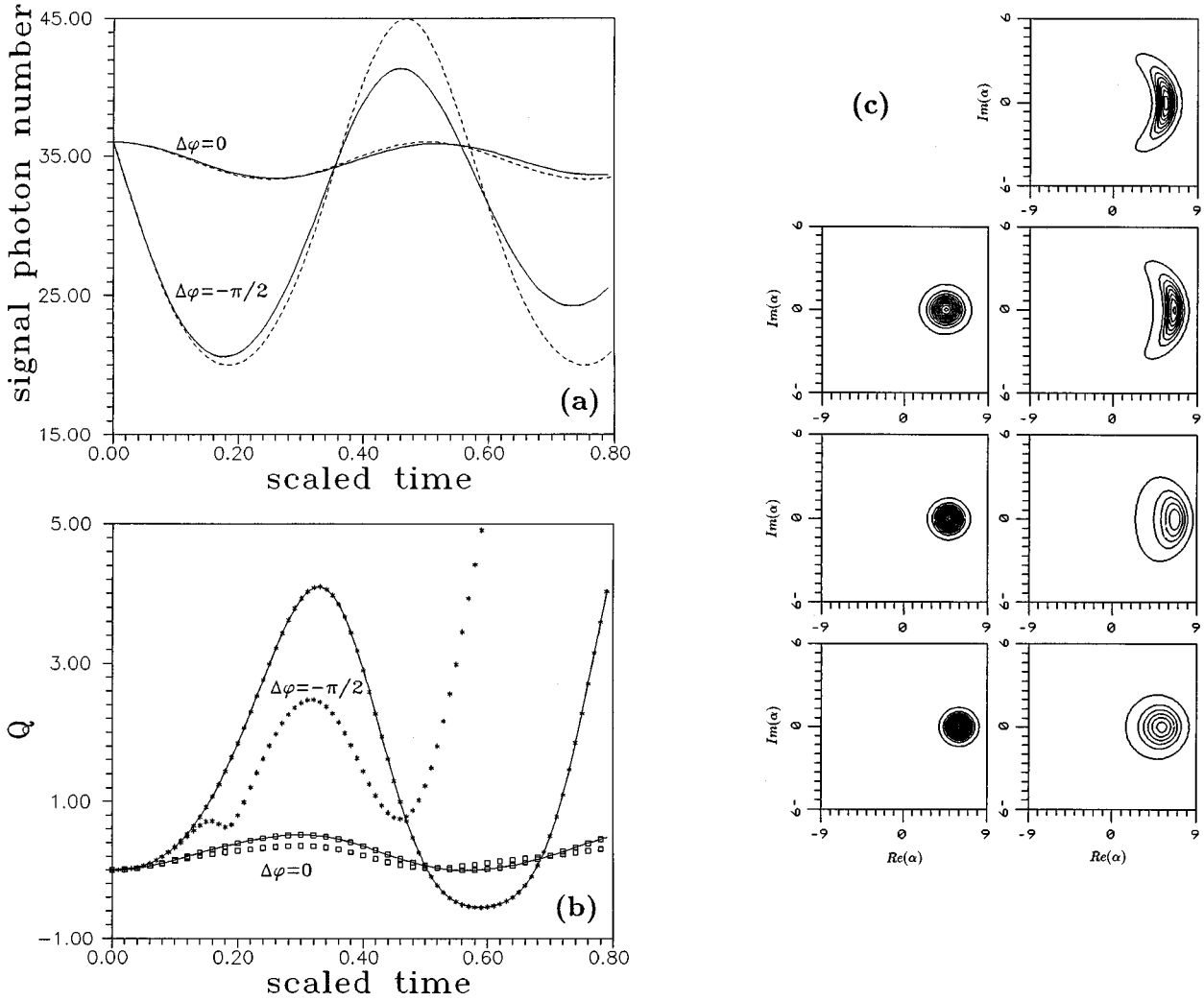

FIG. 1. (a) Change of the signal mean photon number for the initial state (5) ($|\alpha|=6,|\beta|=4,|\gamma|=3$) with $\Delta\varphi=0$ and $\Delta\varphi=-\pi/2$. The full line represents the quantum calculation of (2) while the dashed line shows the classical solution of (9) and (11). In the out-of-phase regime ($\Delta\varphi=0$) we can see clearly the start of the change beginning in second order of time. (b) Q parameter [Eq. (25)] of the signal (joined) and idler for the same initial state as in Fig. 1(a) according to the quantum calculation (2). The most interesting nonclassical phenomenon occurs for the signal at $\Delta\varphi=-\pi/2$, where Q becomes negative after the restart of sum-frequency generation while the Q of the idler shows the opposite tendency. This is due to the different preparations during the first quasiperiod because signal and idler start with the mean photon numbers $|\alpha|^2=36$ and $|\beta|^2=16$, respectively. (c) Contour lines of the Q (quasiprobability) function for the signal wave at the phase difference $\Delta\varphi=-\pi/2$ calculated quantum mechanically at equidistant times [$\Delta(\kappa t)=0.1$]. The center of these lines (starting circularly) moves radially (phase stable). The blowup illustrates the increase of phase and amplitude fluctuations while the deformation and transition to bananalike contours signals first pump saturation and then sub-Poissonian photon statistics, respectively.

Note the virtually complete energy exchange in the out-of-phase regime [Fig. 3(a)] and the remarkable motion of the classical phase difference accompanying it [Fig. 4(a)]. The change of the single phases is made visible by plotting the contour lines of the Q function for the various modes at equidistant times [Fig. 4(b)].

V. KERR-STATE ANSATZ FOR THE SIGNAL MODE

Achieving a remarkable nonclassical effect after one quasiperiod in the three-wave interaction is physically very interesting, but experimentally still unrealistic. Therefore we tried to understand the mechanism of this effect and to find ways to realize it within the first quasiperiod, i.e., before the signal or pump mode are depleted for the first time. One method to get this without any entanglement at the beginning is a Kerr-state ansatz for the signal mode and coherent states for the idler and pump. This uses the properties of a Kerr state [16], that

$$ {}_K\langle\alpha|\hat{a}^{\dagger 2}\hat{a}|\alpha\rangle_K=\alpha^*|\alpha|^2\ \exp\{-|\alpha|^2[1-\cos(\epsilon)] +i|\alpha|^2\ \sin(\epsilon)+i\epsilon\}, \tag{27}$$

while

$$ {}_K\langle\alpha|\hat{a}^{\dagger}|\alpha\rangle_K=\alpha^*\ \exp\{-|\alpha|^2[1-\cos(\epsilon)]+i|\alpha|^2\ \sin(\epsilon)\}, \tag{28}$$

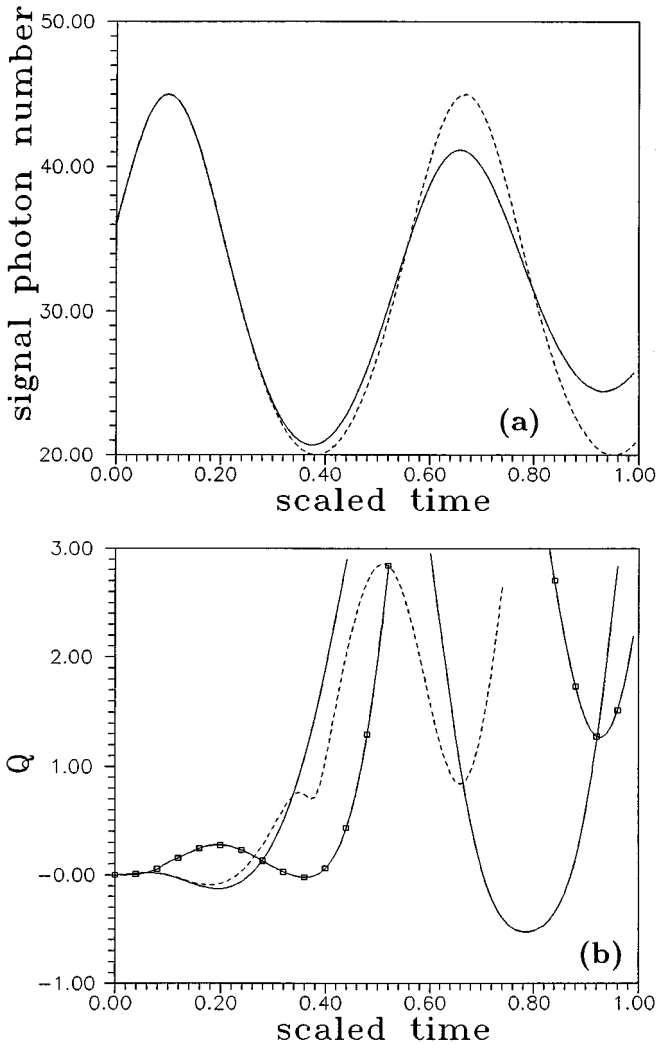

FIG. 2. (a) Same parameters as in Fig. 1(a) but for the case $\Delta\varphi=\pi/2$.(b) Q parameter [Eq. (25)] of the signal (full line), idler (dashed line), and pump (line with squares) for the same case as in (a). After the second start of sum-frequency generation we observe again the remarkable sub-Poissonian photon statistics in the signal.

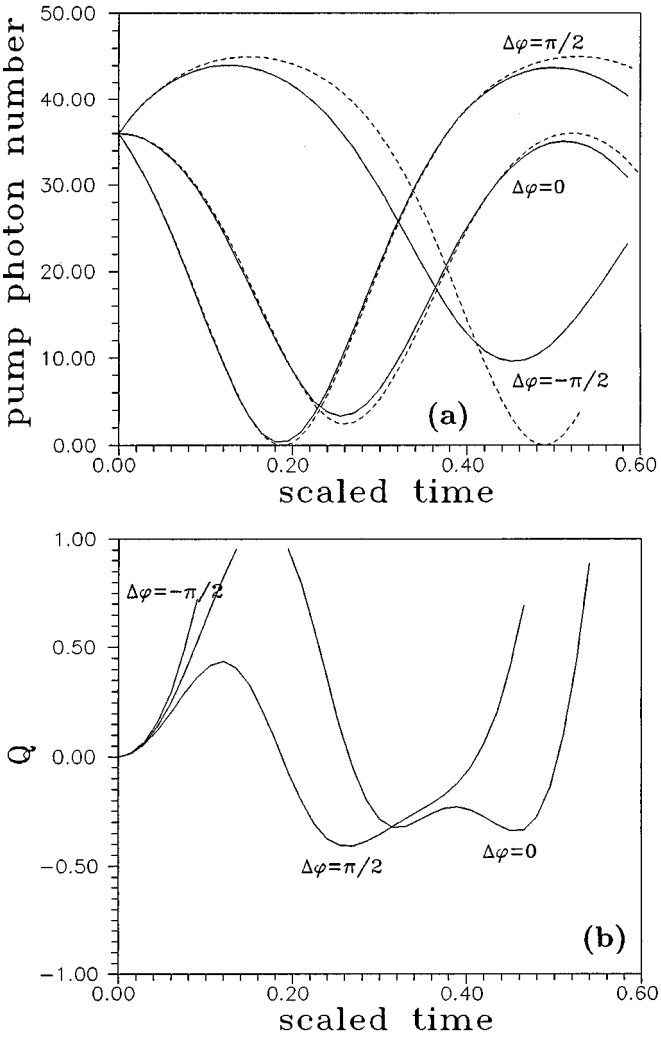

FIG. 3. (a) Change of the pump mean photon number when it starts as the strongest wave ($|\alpha|=4,|\beta|=3,|\gamma|=6$). As in Fig. 1(a), the full line represents the quantum solution while the dashed line corresponds to the classical case. The energy exchange for $\Delta\varphi=0$ is now almost as effective as for the optimum phase differences ($\Delta\varphi=\pm\pi/2$). (b) Q parameter [Eq. (25)] of the signal wave and the same case as in (a). Even in the out-of-phase regime ($\Delta\varphi=0$) there is sub-Poissonian photon statistics during sum-frequency generation after saturated amplification.

where $|\alpha\rangle_K$ is a Kerr state developed from a coherent state and

$$ {}_K\langle\alpha|\hat{a}^\dagger|\alpha\rangle_K=\langle\alpha|\hat{a}^\dagger e^{i\epsilon\hat{a}^\dagger\hat{a}}|\alpha\rangle. \tag{29}$$

In (29) we denote by ϵ a scaled interaction parameter that contains $\chi^{(3)}$ and the interaction length. This equation uses the simple operator solution for the ideal Kerr effect [16].

If we compare (27) and (28) the small phase shift ϵ introduced by the commutation relations becomes very important and leads, for

$$\varphi_a+\varphi_b-\varphi_c-|\alpha|^2\,\sin\epsilon=0, \tag{30}$$

to a nonzero first-order term in the expectation value of (8), while the photon number has no such contribution. The variance of the photon number is then

$$\langle[\hat{a}^\dagger(t)\hat{a}(t)]^2\rangle-\langle\hat{a}^\dagger(t)\hat{a}(t)\rangle^2=|\alpha|^2+\kappa t|\alpha|^3|\beta||\gamma|\sin\epsilon+2\kappa^2t^2|\gamma|^2|\alpha|^2|\beta|^2\{1-\exp[-|\alpha|^2(1-\cos2\epsilon)]\cos\epsilon\}$$
$$+\kappa^2t^2[|\alpha|^2(|\gamma|^2-|\beta|^2)+|\gamma|^2(|\beta|^2+1)+2|\alpha|^2|\gamma|^2]+O(\kappa^3t^3). \tag{31}$$

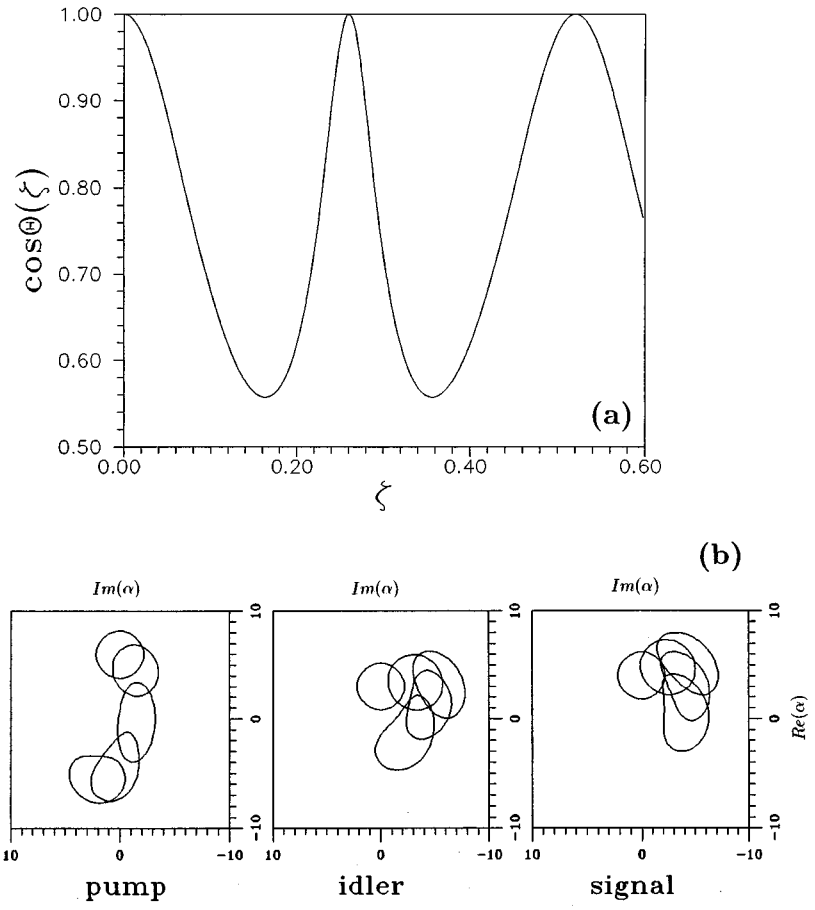

FIG. 4. (a) Behavior of the cosine of the classical phase difference [Eq. (10)] for initially $\Delta\varphi=0$ and the same amplitude parameters as in Fig. 3(a). The variable is the classical coordinate ζ, which corresponds exactly to the scaled time κt. (b) Illustration of the phase motion by contour lines of the Q function within the quantized model and $\Delta\varphi=0$. The amplitudes are the same as in Fig. 3(a). For clarity we plot only one contour line at the equidistant times $[\Delta(\kappa t)=0.13]$ with the height 0.01. The shift of the pump phase is initially the smallest because this wave is the most intense.

This equation shows for $\epsilon<0$ a strong tendency to sub-Poissonian statistics because only in (31) is there such a contribution of first order in κt for the phase relation (30) while the photon number stays constant in first order.

The disappearance of the first-order terms in (6) with the Kerr state in the signal and the phase difference (30) means that

$$\langle\hat{a}\rangle_K\langle\hat{b}^\dagger\hat{c}\rangle-\langle\hat{a}^\dagger\rangle_K\langle\hat{c}^\dagger\hat{b}\rangle=0$$

and is thus equivalent to a vanishing field strength in the Kerr state. The coherent states in the idler and pump can namely be thought of as determining the phase position of the electric field in the signal. A vanishing Kerr field strength is exactly the condition for obtaining extreme sub-Poissonian statistics by interference of a coherent beam and a Kerr-state field [17]. Note also that a Kerr state at this phase position cannot show any squeezing.

In Fig. 5(a) we plot the Q parameter [Eq. (25)] of the signal for the interaction (2) and the initial state $|\alpha=6\rangle_K|\beta=4\rangle_b|\gamma=3\rangle_c$ imposing the phase relation (30). A very short interaction time is sufficient to result in a strong sub-Poissonian photon statistics. On the other hand, the extremes obtained by interference [16,17] cannot be reached because the phases move classically in this configuration out of the position $\Delta\varphi=0$. This is illustrated in Fig. 5(b). We should mention that we get a similar result if we start with $|\alpha=4\rangle_K|\beta=3\rangle_b|\gamma=6\rangle_c$, but now with an initial amplification of the signal for $\Delta\varphi=0$ because the intensity relations here lead to a positive term of second order in time in (6).

In the optimized interference version of Kitagawa and Yamamoto [17] the photon number in the output is increased by a relatively small amount from the coherent reference field. This field shifts the Q function of the Kerr state in an optimum position between concentric circles and so the photon-number fluctuations attain their minimum.

VI. PREPARED ENTANGLEMENT BETWEEN THE SIGNAL AND PUMP

With our knowledge about the parametric interaction on a Kerr state in the signal mode we return to the results in Figs. 1(a)–1(c). There is of course no Kerr effect at the restart of sum-frequency generation, although the phase fluctuations are enhanced after this saturated amplification process (cf. [18]). But our Kerr-state calculations teach us that there must be a first-order of time reduction effect of the photon-number variance. However, this is not conceivable in a disentangled state because at this moment we have

$$\langle\hat{c}\rangle=\langle\hat{c}^\dagger\rangle=0, \tag{32}$$

i.e., the coherent pump amplitude crosses zero. In addition, the signal and idler photon numbers are maximum, i.e., the first derivative of the mean signal photon number vanishes

$$\frac{d}{dt}\langle\hat{a}^\dagger\hat{a}\rangle=\frac{i}{\hbar}\langle[\hat{H}_{\rm int},\hat{a}^\dagger\hat{a}]\rangle=i\kappa\langle(\hat{a}\hat{b}\hat{c}^\dagger-\hat{a}^\dagger\hat{b}^\dagger\hat{c})\rangle=0,$$

which amounts to

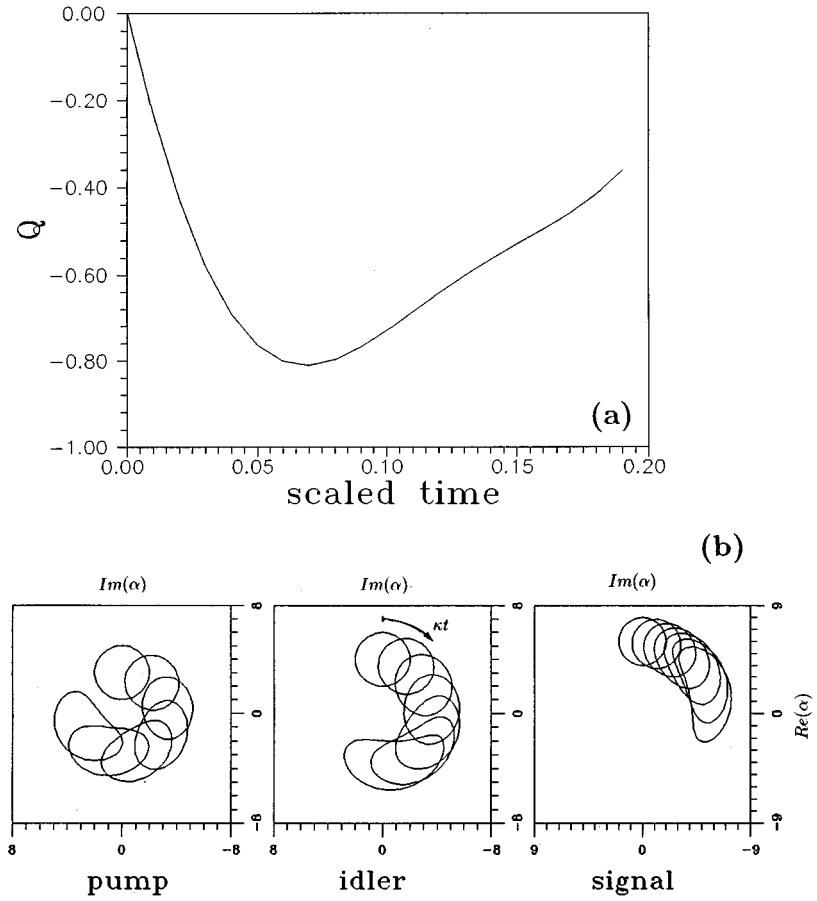

FIG. 5. (a) Q parameter [Eq. (25)] of the signal as a function of time for the Kerr-state ansatz in the signal and coherent states in the idler and pump. The amplitudes are $|\alpha|=6$, $|\beta|=4$, and $|\gamma|=3$ and the phases fulfill Eq. (30) with $\epsilon=-0.1$. The strong tendency to negative values described by Eq. (31) leads to a fast decrease of Q, but the classical phase shifts present at $\Delta\varphi=0$ and illustrated in (b) limit the achievable minimum. (b) Illustration of the classical phase shifts for the initial state (5) by Q-function contour lines at equidistant times $[\Delta(\kappa t)=0.1]$ for the same amplitude parameters as in (a). For clarity we plot only one contour line at each time with the height 0.01. These nonlinear phase shifts are typical for the out-of-phase regime $\Delta\varphi=0$. The initial photon numbers are close to the case where classically no energy exchange takes place. The time flow in all cases is indicated by an arrow in the idler picture.

$$\langle \hat{a}\hat{b}\hat{c}^{\dagger}\rangle=\langle \hat{a}^{\dagger}\hat{b}^{\dagger}\hat{c}\rangle, \tag{33}$$

and hence the mean values are real. The simple consequence of Eq. (33) is that there is no first-order contribution to the signal photon number as well as to any other of the modes due to the conservation laws. In addition, we are working in the phase-stable regime with $\Delta\varphi=-\pi/2$, which implies $\Gamma=0$. This means that the expectation value of the interaction Hamiltonian $\hat{H}_{\rm int}$ also equals zero

$$\langle \hat{H}_{\rm int}\rangle=\hbar\kappa\Gamma=\hbar\kappa(\langle \hat{a}\hat{b}\hat{c}^{\dagger}\rangle+\langle \hat{a}^{\dagger}\hat{b}^{\dagger}\hat{c}\rangle)=0.$$

As a consequence, at the moment of maximum photon number in the signal we have

$$\langle \hat{a}\hat{b}\hat{c}^{\dagger}\rangle=0.$$

Because the signal and the idler are strongly populated and have a considerable coherent amplitude at this moment, the vanishing of the mean value $\langle \hat{a}\hat{b}\hat{c}^{\dagger}\rangle$ can only be due to the zero crossing of the pump amplitude as expressed in Eq. (32). Our numerical results show exactly the coincidence of both zeros. The dynamics of the pump is illustrated in Fig. 6. The initial coherent state at the moment $t=0$ is first amplified and then attenuated. The attenuation is seen as the approach to the zero point $[\mathrm{Re}(\alpha)=0,\mathrm{Im}(\alpha)=0]$ along a straight line (phase-stable motion) and then is amplified again by crossing the center. Note also that the zero crossing of the quantity Eq. (33) induces a phase shift, making possible the reverse of the energy exchange process, i.e., the buildup of the pump. As already mentioned, the simultaneous zero crossing of the pump amplitude does not imply a possible factorization of the total state vector of the three-mode system. It means only that both crossings are not mu-

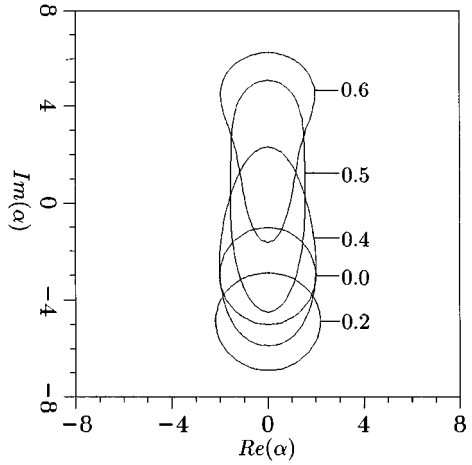

FIG. 6. Dynamics of the pump in the regime of phase stable motion $\Delta\varphi=-\pi/2$ $(\Gamma=0)$. The amplitudes of the modes have been set as in Fig. 1(a). To avoid confusing overlaps of the (outer) contour lines we do not plot all time moments. The pump is first amplified (contour line at $\kappa t=0.2$) and then attenuated ($\kappa t=0.4$) and amplified again ($\kappa t=0.6$). During this process the mean value of the pump amplitude crosses zero (near to $\kappa t=0.5$), although (due to considerable fluctuations) the mean photon number is not zero at this moment.

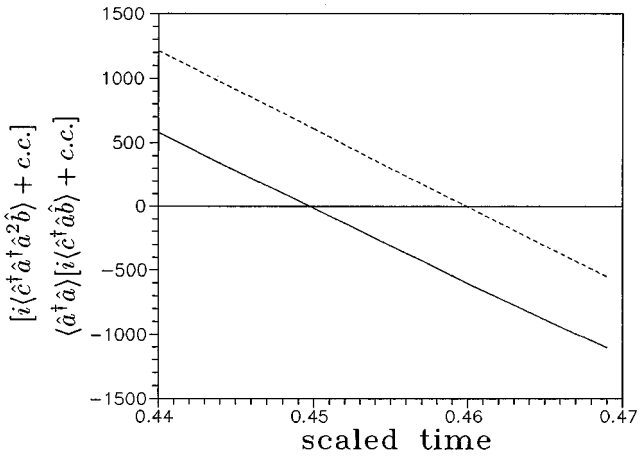

FIG. 7. Behavior of $[i\langle\hat{c}^\dagger\hat{a}\hat{b}\rangle + \text{c.c.}]\langle\hat{a}^\dagger\hat{a}\rangle$ (dashed line) and of $[i\langle\hat{c}^\dagger\hat{a}^\dagger\hat{a}^2\hat{b}\rangle + \text{c.c.}]$ (full line) at the restart of sum-frequency generation in Figs. 1(a) and 1(b) ($\Delta\varphi = -\pi/2$). The process begins where the first quantity crosses zero. The second is then negative and describes the tendency to sub-Poissonian photon statistics in the expectation value of Eq. (8).

tually shifted by any correlations. Finally, it is important to notice that the following quantity is nonzero:

$$i\langle\hat{c}^\dagger\hat{a}^\dagger\hat{a}^2\hat{b}\rangle - i\langle\hat{b}^\dagger\hat{a}^{\dagger 2}\hat{a}\hat{c}\rangle < 0 \tag{34}$$

at the zero crossing discussed above. Equation (34) in turn has the consequence that there is a first-order term in the photon-number variance.

If we had factorized the expectation values in (34) we would always get zero due to condition (32). So it follows that the entanglement between the pump and signal is crucial for the presence of a strong tendency to sub-Poissonian photon statistics in the signal mode. The behavior of the quantity (34) in comparison to (33) multiplied by the photon number is shown in Fig. 7 for a region around the second start of the sum-frequency generation.

Now by seeing the effect of (34) we conclude that it results from the preparation in the first quasiperiod. In this sense the first quasiperiod can be interpreted as a state preparation for a special sum-frequency generation. During this period the nonlinear amplification of the signal and idler up to the exhaustion of the pump wave is most important. It starts linearly when the idler amplitude crosses zero (more exactly when $\langle\hat{a}\hat{b}\rangle = 0$) and becomes nonlinear insofar as the number fluctuations in the signal are then reduced while the signal phase fluctuations continue to grow, as illustrated in Fig. 1(c). These findings with respect to the phase agree with those obtained in [18].

VII. SOME PROPERTIES OF THE PARAMETRIC APPROXIMATION

We have already mentioned that certain properties survive the transition in which the pump wave becomes very strong and is not affected by the energy transfer from or to the signal and idler. The pump wave is then treated as a classical c number and any depletion is neglected. In the interaction picture the solutions for the signal and idler are then [3]

$$\hat{a}(T) = \hat{a}\,\cosh(T) + \hat{b}^\dagger i\,\sinh(T),$$

$$\hat{b}(T) = \hat{b}\,\cosh(T) + \hat{a}^\dagger i\,\sinh(T), \tag{35}$$

where the operators are defined as in Sec. II and T contains the coupling constant and the pump amplitude. The phase scaling is as in [3]. To simplify the expressions we will use the abbreviations

$$\cosh(T) = c(T), \quad \sinh(T) = s(T).$$

With (35) we find for the signal photon number for initially coherent states $|\alpha\rangle_a$ in a and $|\beta\rangle_b$ in b (as in Sec. II)

$$\langle\hat{a}^\dagger(T)\hat{a}(T)\rangle = |\alpha|^2c^2(T) + 2|\alpha||\beta|s(T)c(T) \times\cos(\pi/2 - \varphi_a - \varphi_b) + (|\beta|^2+1)s^2(T), \tag{36}$$

from which we see that, in [3], φ_c is set equal to π.

In discussing various simple cases let us first assume that $|\alpha| = 4$, $|\beta| = 3$, and

$$\varphi_c - \varphi_a - \varphi_b = \pi - \varphi_b - \varphi_a = 0, \tag{37}$$

i.e., we consider the out-of-phase regime in the parametric approximation. The photon number (36) will then always increase because the pump photon number is sufficiently large and therefore the second-order term in (6) is always positive. Concerning the signal amplitude we find

$$\langle\hat{a}(T)\rangle = 2e^{i\varphi_a}(e^T + e^{-T}) + \tfrac{3}{2}e^{i(\pi/2-\varphi_b)}(e^T - e^{-T})$$

$$= e^{i\varphi_a}[(2 - \tfrac{3}{2}i)e^T + (2 + \tfrac{3}{2}i)e^{-T}], \tag{38}$$

where we used (37). The equivalent result for the idler mode is

$$\langle\hat{b}(T)\rangle = e^{i\varphi_b}[(\tfrac{3}{2} - 2i)e^T + (\tfrac{3}{2} + 2i)e^{-T}]. \tag{39}$$

These two equations tell us that there are phase shifts for the signal and idler that amount, for strong amplification, to rotations by 36.9° and 53.1°, respectively. We can see these rotations qualitatively in Fig. 4(b), where the pump wave contained initially 36 photons as the strongest wave. For a more exact agreement we would need a much stronger pump wave. Thus there are phase shifts within the parametric approximation.

Our other example refers to the first zero passage of the idler amplitude (and of $\langle\hat{c}^\dagger\hat{b}\hat{a}\rangle$) for $\Delta\varphi = -\pi/2$ in Fig. 1(a). After this phase jump by π of the idler wave both the signal and idler are amplified until the complete depletion of the pump. The zero passage of the idler has an analog in the parametric approximation and the number fluctuations can here be calculated to

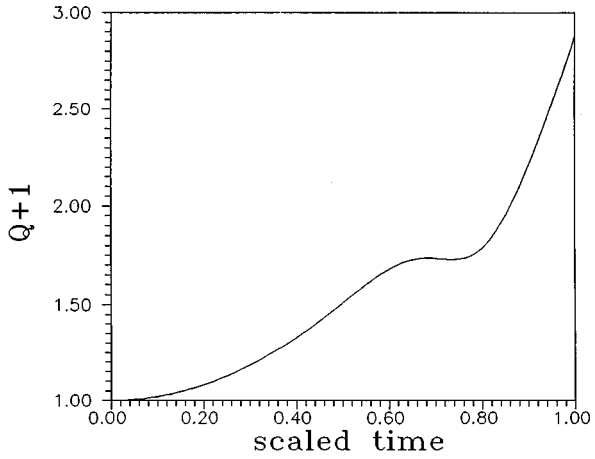

FIG. 8. Relative photon-number fluctuations [Eq. (25)] of the idler wave with a very strong pump wave (parametric approximation) in the damping regime ($\Delta\varphi=-\pi/2$). The wiggle appears where the idler amplitude crosses zero.

$$\frac{\langle[\hat{b}^\dagger(T)\hat{b}(T)]^2\rangle-\langle\hat{b}^\dagger(T)\hat{b}(T)\rangle^2}{\langle\hat{b}^\dagger(T)\hat{b}(T)\rangle}$$

$$=c^2(T)+s^2(T)\frac{[|\beta|c(T)-|\alpha|s(T)]^2}{\langle\hat{b}^\dagger(T)\hat{b}(T)\rangle}. \qquad (40)$$

The fluctuations (40) are plotted in Fig. 8 for the case $|\alpha|=6$, $|\beta|=4$, and $\Delta\varphi=-\pi/2$ and show qualitatively the same wiggle as in Figs. 1(b) and 2(b) (Q_b of the idler).

VIII. CONCLUDING REMARKS

We have presented a classical and quantum-mechanical analysis of the three-wave interaction in its simplest form without any losses, but including the full quantization of all three modes and depletion. Already in this idealized description there is a variety of effects that demand further investigation and offer interesting experimental possibilities.

Our numerical calculation starts with sufficiently strong coherent states in all three modes and therefore allows us to investigate all possible phase regimes. In general, the single phases and their difference change during the interaction. Exceptions can be found only for distinguished phase differences or initially empty modes.

There is a close analogy between the quantum and classical behavior because the conserved quantities are equivalent. On the other hand, we can find drastic differences due to the developing entanglement between the modes, which has no classical analog.

Besides the well-known entanglement between the signal and idler, there can also be an entanglement between the signal and the pump mode after saturated amplification of the signal. This entanglement is responsible for the strong nonclassical effects during sum-frequency generation in the nondegenerate process where normally nothing unexpected is happening.

The entanglement is usually indicated by the purity of the modes, but here we have focused on certain expectation values that could not be factorized. The study of these expectation values showed strong tendencies to nonclassical effects that were proved by our numerical analysis to last during longer interaction times.

[1] P. Franken, A. E. Hill, C. W. Peters, and G. Weinreich, Phys. Rev. Lett. **7**, 118 (1961).
[2] J. A. Armstrong, N. Bloembergen, J. Ducuing, and P. S. Pershan, Phys. Rev. **127**, 1918 (1962).
[3] B. R. Mollow and R. J. Glauber, Phys. Rev. **160**, 1076 (1967); **160**, 1097 (1967).
[4] Z. Y. Ou, S. F. Pereira, and J. H. Kimble, Phys. Rev. Lett. **70**, 3239 (1993).
[5] L. J. Wang, X. Y. Zou, and L. Mandel, J. Opt. Soc. Am. B **9**, 605 (1992), and references therein.
[6] M. Hillery and M. S. Zubairy, Phys. Rev. A **29**, 1275 (1984); M. Hillery, Daoqi Yu, and J. Bergou, *ibid.* **49**, 1288 (1994).
[7] J. Opt. Soc. Am. B **4** (10), 1453 (1987), special issue on squeezed states of the electromagnetic field, edited by H. J. Kimble and D. F. Walls; J. Mod. Opt. **34** (6,7), 709 (1987), special issue on squeezed states, edited by R. Loudon and P. L. Knight.
[8] D. F. Walls and R. Barakat, Phys. Rev. A **1**, 446 (1970).
[9] P. Carruthers and M. M. Nieto, Phys. Rev. Lett. **14**, 387 (1965).
[10] H. Paul, *Nichtlineare Optik II* (Akademie-Verlag, Berlin, 1973). In the degenerate case (second-harmonic generation), there are additional factors; see p.10.
[11] A. Bandilla, G. Drobný, and I. Jex (unpublished).
[12] *Handbook of Mathematical Functions*, edited by M. Abramowitz and I. A. Stegun (Dover, New York, 1964).
[13] D. Pegg and S. M. Barnett, Phys. Rev. A **39**, 1665 (1989).
[14] G. Drobný and I. Jex, Czech. J. Phys. **44**, 827 (1994).
[15] A. Bandilla, G. Drobný, and I. Jex (unpublished).
[16] H.-H. Ritze and A. Bandilla, Opt. Commun. **29**, 126 (1979).
[17] M. Kitagawa and Y. Yamamoto, Phys. Rev. A **34**, 3974 (1986).
[18] M. J. Collett and D. F. Walls, Phys. Rev. Lett. **61**, 2442 (1988).